

Supplementary Information for

**Fluorescent nanoparticles based on microporous organic polymer network:
fabrication and efficient energy transfer to surface-bound dyes**

Abhijit Patra^{*}, Jan-Moritz Koenen and Ullrich Scherf

CONTENTS

Pages

2 – 6	I. Synthesis and Characterization (a) Chemicals and general methodology (b) Fabrication of nanoparticles by miniemulsion polymerization
7 – 8	II. Details of size distribution and morphology (a) Fabrication of samples (b) Scanning electron microscopy and size distribution histogram (c) Atomic force microscopy
9 – 11	III. Spectroscopic data (a) Absorption spectrum of thin film of nanoparticles (b) Emission and excitation spectra
12	References

I. Synthesis and Characterization

Instrumentation: ^1H - and $^{13}\text{C}\{^1\text{H}\}$ -NMR spectra were recorded on a Bruker Avance III 600 spectrometer. The chemical shifts (δ) are reported in parts per million (ppm) using residual solvent signals as internal standards. FTIR measurements were accomplished on a Jasco FT/IR-4200 spectrophotometer. Fifty scans were signal-averaged, with a resolution of 4 cm^{-1} at room temperature. Direct powdered solid was used for the measurements in ATR mode. Ultrasonication was carried out with Branson sonifier (model: W-450 classic) using microtip of 5 mm tip diameter.

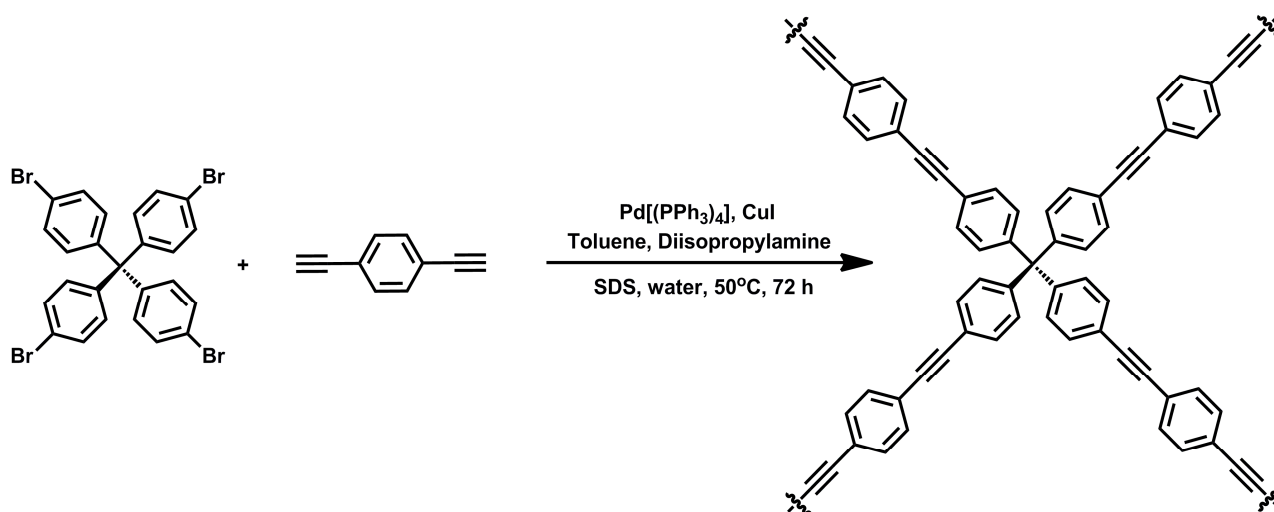
(a) Chemicals: All chemicals were used as received unless stated otherwise. Triphenylmethanol (97%), isopentyl nitrite (97%) and bromine (99.5%) were received from Sigma-Aldrich. Tetrakis(triphenylphosphine)palladium (99.9%) was obtained from Strem Chemicals. Aniline (99%) was procured from Merck. Copper(I) iodide (99.995%), bis(triphenylphosphine)palladium(II) dichloride (98%), sodium dodecyl sulfate (99%), toluene (99.85%), diisopropylamine (99%), 1,2-dichloroethane and 50 wt% solution of hypophosphorous acid in water were received from Acros Organics. Triethylamine (99.5%), Ethanol (99.8%), extra pure conc. HCl, conc. H_2SO_4 and glacial acetic acid were received from Carl Roth GmbH. 1,4-diethynylbenzene (95%) obtained from Acros Organics was further purified by washing through a silica gel column and subsequent recrystallizations.

Tetrakis(4-bromophenyl)methane was synthesized starting from triphenylmethanol following a reported procedure.¹

Sonogashira cross-coupling polycondensation between tetrakis(4-bromophenyl)methane and 1,4-diethynylbenzene using bis(triphenylphosphine)palladium(II) dichloride as catalyst and copper(I) iodide as co-catalyst in a solvent mixture of toluene and triethylamine was performed following a reported procedure.² Purified and dried network was found to show similar ^1H - ^{13}C cross-polarization (CP) MAS NMR spectrum[†] as reported earlier.³

[†] We gratefully acknowledge Dr. Michael Ryan Hansen of MPIP, Mainz for ^1H - ^{13}C cross-polarization (CP) MAS NMR measurement.

(b) **Polymerization in a Miniemulsion State: *in situ* fabrication of nanoparticles:**



Scheme S1: Synthesis of nanoparticles composed of a tetraphenylmethane-based microporous organic polymer (TPM-MOP).

Direct polymerization to nanoparticles was achieved following minor modification of the procedure reported for the fabrication of conjugated polymer nanoparticles by miniemulsion polymerization.⁴ In a 100 mL schlenk tube, 500 mg sodium dodecyl sulfate (SDS) was dissolved in 50 mL of degassed water. Tetrakis(4-bromophenyl)methane (0.130 g, 0.2 mmol), 1,4-diethynylbenzene (0.075 g, 0.6 mmol), Tetrakis-(triphenylphosphine)palladium (0.0023 g, 0.002 mmol) and copper(I) iodide (~. 100 μ g) were taken in a glass tube and sealed under argon atmosphere with a septum. Freshly distilled toluene (1.4 ml) and diisopropylamine (0.7 ml) were added to the reactant mixture; solids were dissolved by stirring and sonication using an ultrasound bath. Then the mixture was added to the surfactant solution under gentle stirring. After stirring vigorously for 15 min for pre-emulsification, the mixture was ultrasonicated for 2 min under argon flow, yielding a stable miniemulsion. Gentle stirring of the miniemulsion at 50°C under Ar atmosphere for 3 days produced a colloidally stable dispersion. This dispersion was stirred, open to air, for 1 day and filtered over sintered glass crucible.

An aliquot of nanoparticle dispersion was precipitated by addition to excess methanol and collected after washing with water, followed by ultracentrifugation, dried and used for FTIR and NMR characterizations.

IR spectroscopy: The FTIR spectrum of TPM-MOP nanoparticles show characteristic bands at 3291 and 2108 cm^{-1} corresponding to $\equiv\text{C}-\text{H}$ and $\text{C}\equiv\text{C}$ stretching indicating coupling between tetrakis(4-bromophenyl)methane

and 1,4-diethynylbenzene. Absorption at 3033 cm^{-1} is assigned to $C_{Ar}\text{-H}$ stretching and aromatic ring ($C=C$) stretching bands are observed at 1508 and 1485 cm^{-1} . Strong bands in the region of $834 - 810\text{ cm}^{-1}$ can be attributed to $C\text{-H}$ bending of *para*-di-substituted benzene ring. Additional bands in the region of $2921 - 2851\text{ cm}^{-1}$ are due to aliphatic $C\text{-H}$ stretching originating from SDS attached to the surface of nanoparticles. Close similarity of the FTIR spectrum in the finger print region of bulk solid obtained by polymerization in the solution state and that of the nanoparticles suggests similar network structure in the nanoparticles as that in the solid.

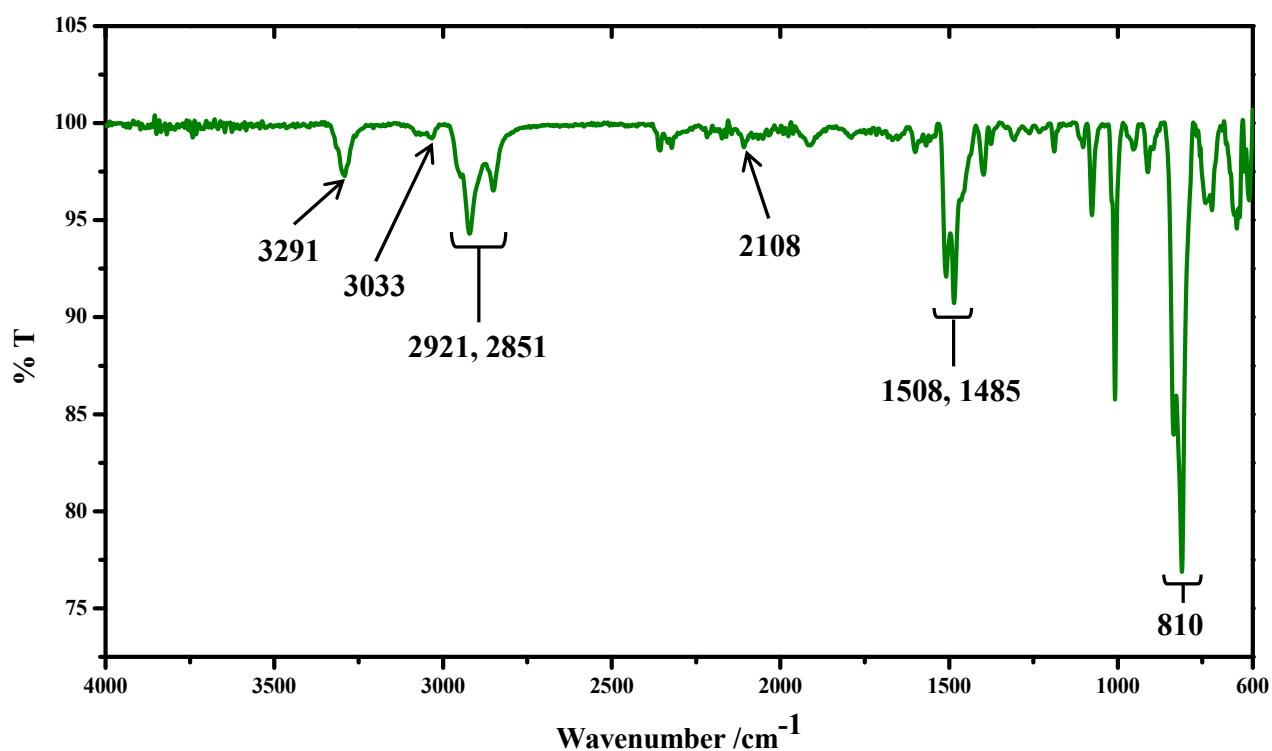


Fig. S1. FTIR spectrum of nanoparticles composed of a tetraphenylmethane-based microporous polymer network.

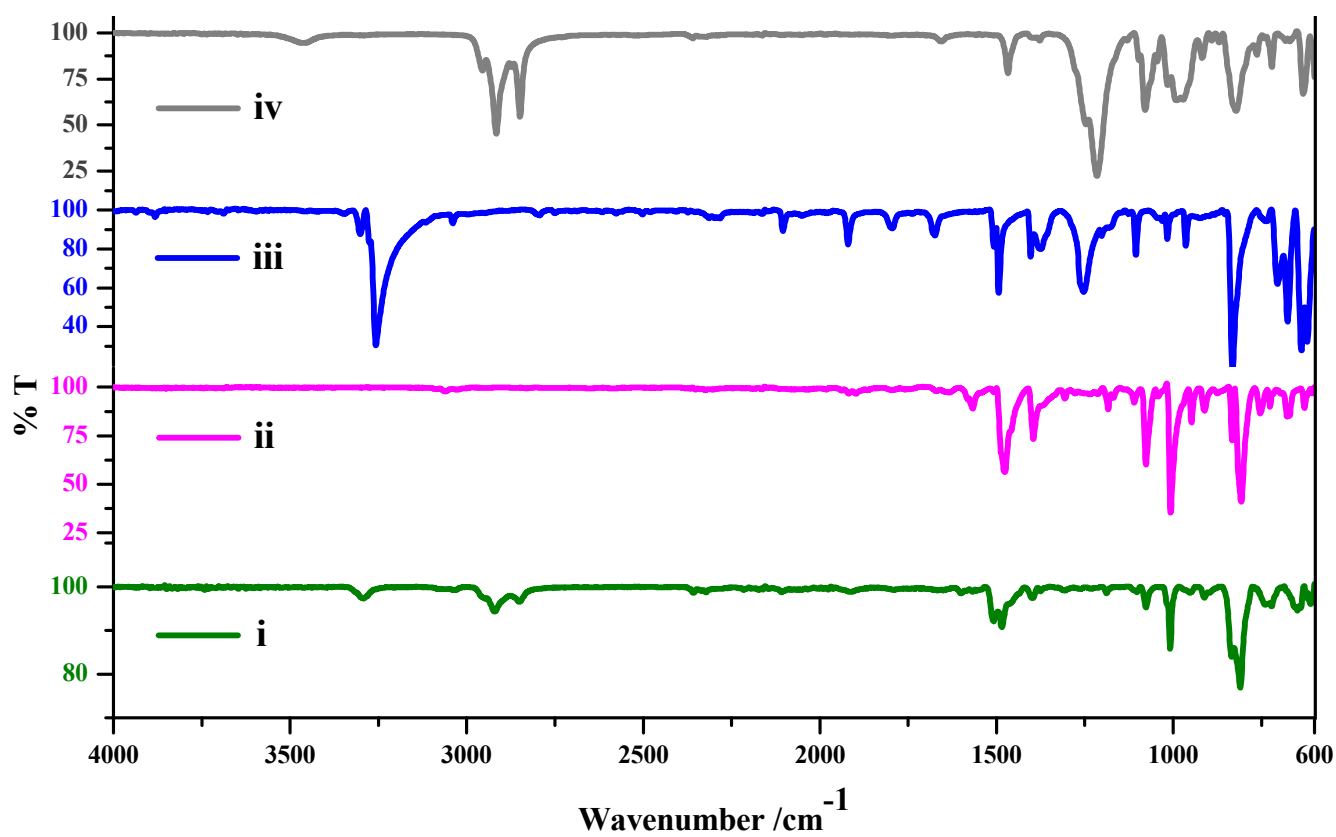


Fig. S2. FTIR spectra of (i) TPM-MOP nanoparticles, (ii) tetrakis(bromophenyl)methane, (iii) 1,4-diethynylbenzene and (iv) SDS.

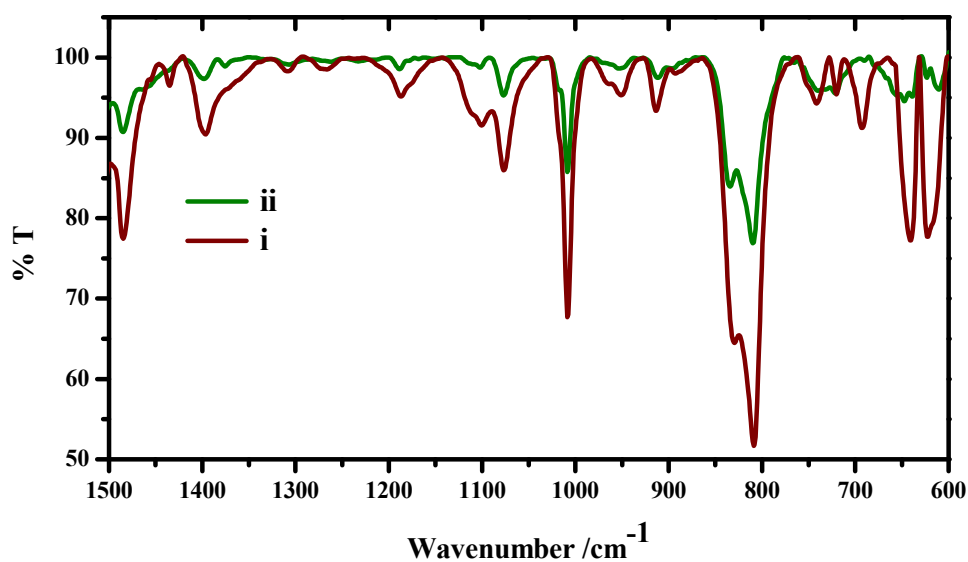


Fig. S3. Finger print regions of FTIR spectra of (i) TPM-MOP in the bulk solid state and (ii) TPM-MOP nanoparticles.

NMR spectroscopy: ^1H NMR spectrum of dilute colloidal dispersion of nanoparticles in $\text{C}_2\text{D}_2\text{Cl}_4$ shows broad signals in the aromatic region. Comparison of ^1H NMR spectrum with that of constituent monomers clearly indicates similar resonances in the nanoparticle dispersion in addition to other resonances, thus demonstrating polycondensation between the monomers. The signal at 3.16 ppm belongs to acetylenic protons of $\text{Ar}-\text{C}\equiv\text{CH}$ end groups. The ratio of intensities of acetylenic protons to aromatic protons is $\sim 1:60$, indicating the presence of one end group for two tetrahedral carbon atoms.

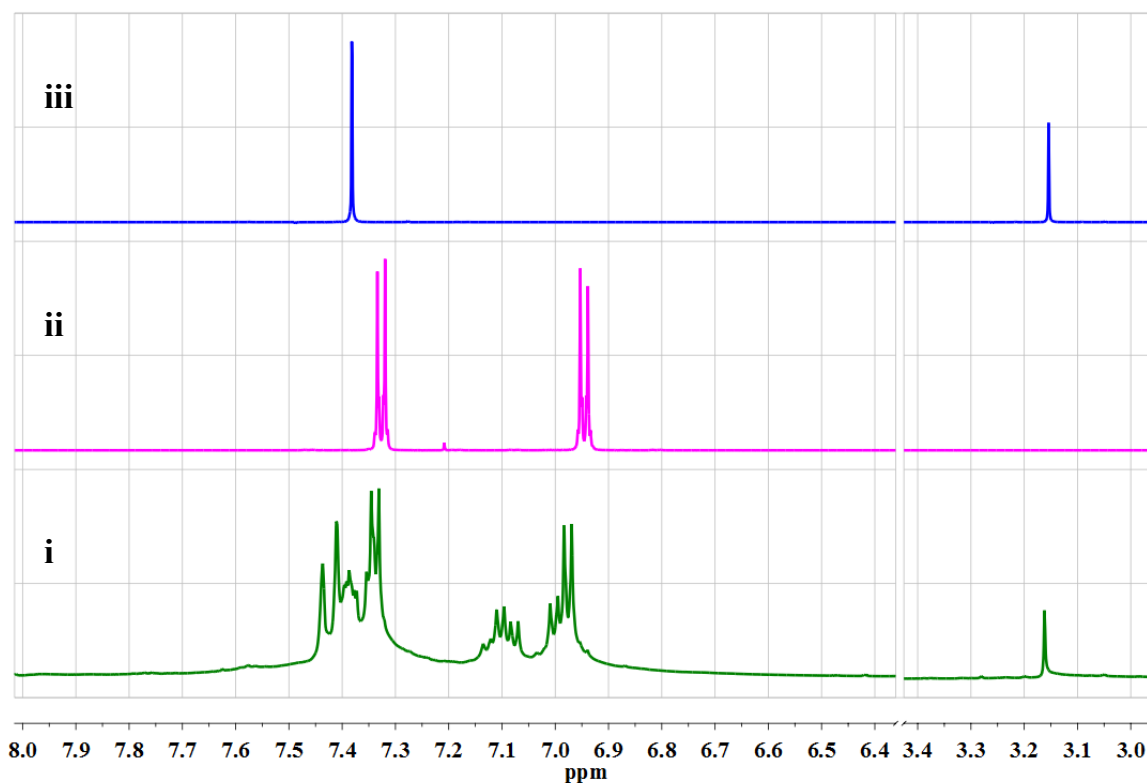


Fig. S4. ^1H NMR spectra of (i) TPM-MOP nanoparticles, (ii) tetrakis(4-bromophenyl)methane and (iii) 1,4-diethynylbenzene.

II. Details of size distribution and morphology

Instrumentation: The size and morphology of the nanoparticles were examined using (a) Philips XL30S scanning electron microscope (SEM) and (b) Bruker di Innova atomic force microscope (AFM). Microscopy was carried out using a beam voltage of 10-12 kV. AFM was done in tapping mode using a silicon non-contact probe (tip radius < 10 nm) having a force constant of 3 N/m. The scanner allowed 90 μm displacements in X-Y direction corresponding to the substrate plane.

(a) Fabrication of samples: The samples for the SEM investigations were collected either on a 20 nm pore alumina membrane (Whatman, Anodisc 13) through filtration of the colloidal solution or deposited on Si wafer by drop casting. The samples prepared on alumina membrane were coated with a thin layer of sputtered gold prior to imaging. Colloidal solution was spin coated on quartz plate to prepare samples for AFM investigations.

(b) Scanning electron microscopy: A size distribution histogram was constructed by measuring particle sizes (more than 100 particles considered) obtained from several SEM images. It was observed that average particle size ranges from 30 to 60 nm indicating fairly uniform distribution of TPM-MOP nanoparticles.

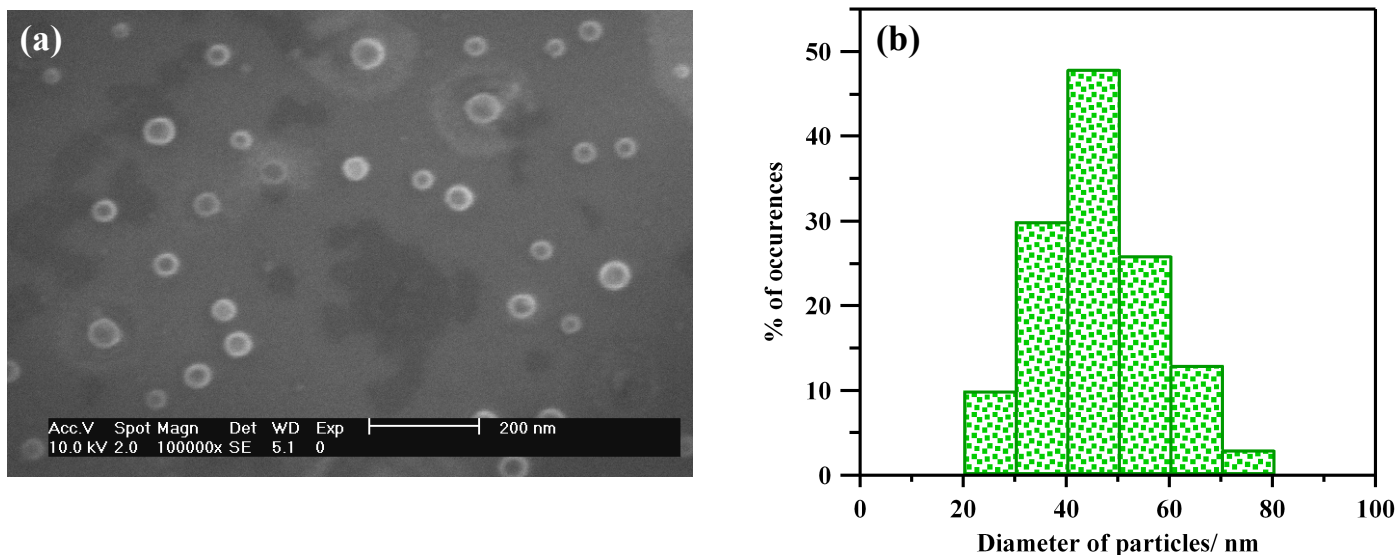


Fig. S5. (a) SEM image of TPM-MOP nanoparticles deposited on Si wafer. (b) Size distribution histogram using SEM images.

(b) Atomic force microscopy

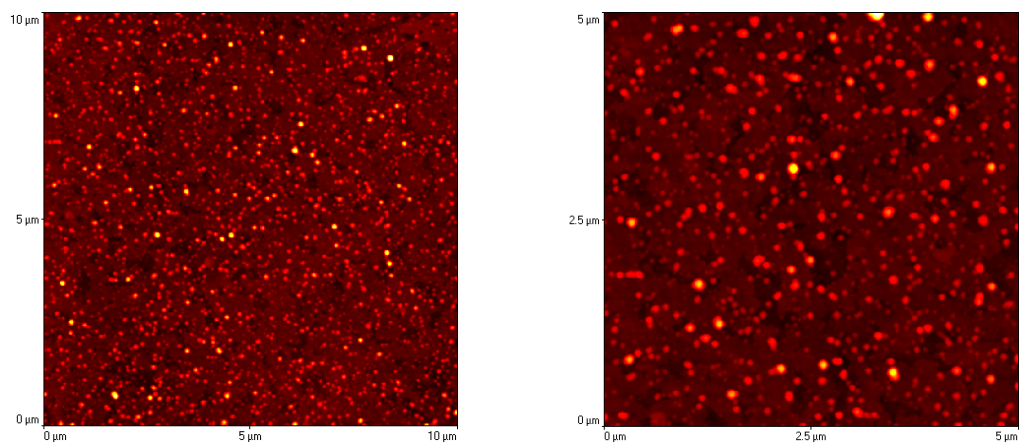


Fig. S6. AFM images of TPM-MOP nanoparticles depicting distribution over a larger area.

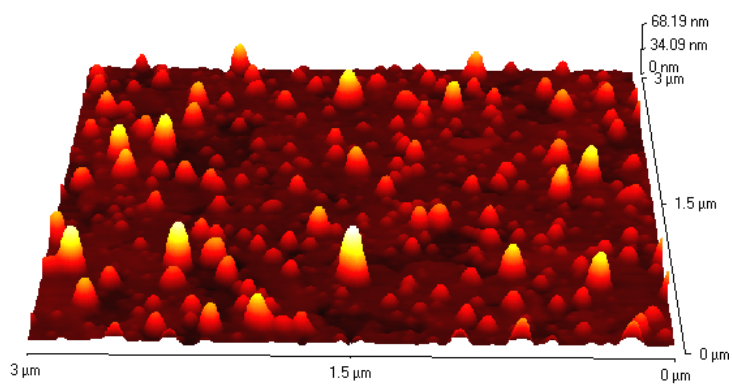


Fig. S7. 3-dimensional topography image of TPM-MOP nanoparticles.

III. Spectroscopic data

Instrumentation: UV-Vis absorption spectra were recorded on a Jasco V550 spectrophotometer. Fluorescence measurements were carried out on a Varian Cary Eclipse spectrofluorimeter.

(a) Absorption spectroscopy: Nanoparticle dispersion was diluted with ultrapure water (Millipore MilliQ, resistivity = 18 M Ω cm) prior to spectroscopic measurements. It was ensured that the optical density is low enough to avoid artifacts due to inner-filter effects.

Thin films of nanoparticles were prepared by spin coating a dilute colloidal dispersion on a quartz plate. These films also showed characteristic absorption peaks with λ_{max} at 311 nm and weak shoulder peaks at 331 and 363 nm as that were observed for the colloidal dispersion. These films were used for AFM analysis.

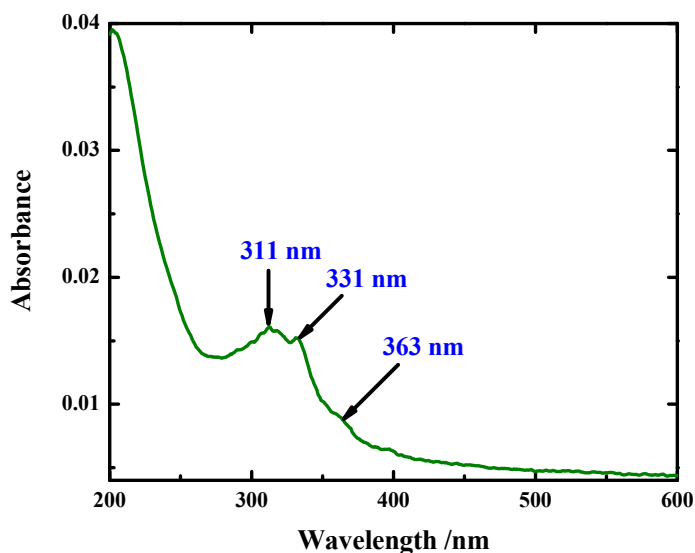


Fig. S8. Absorption spectrum of the thin film of TPM-MOP nanoparticles.

(b) Fluorescence spectroscopy: Emission of nanoparticle dispersion was investigated by exciting at different excitation wavelengths. It was observed that the basic spectral features are the same with peak maximum at 505 nm. The variation of fluorescence intensity with the excitation wavelengths is due to the difference in optical densities at those wavelengths. It was also found that the excitation spectrum resembles to the absorption spectrum and excitation spectra are independent of the wavelengths of emission monitored. This suggests that the emission is likely to be from the same state to which the molecules are vertically excited.

The fluorescence quantum yield of the colloidal dispersion of TPM-MOP nanoparticles was estimated by comparison with quinine sulfate in 1N H₂SO₄ ($\Phi_f = 0.546$).⁵

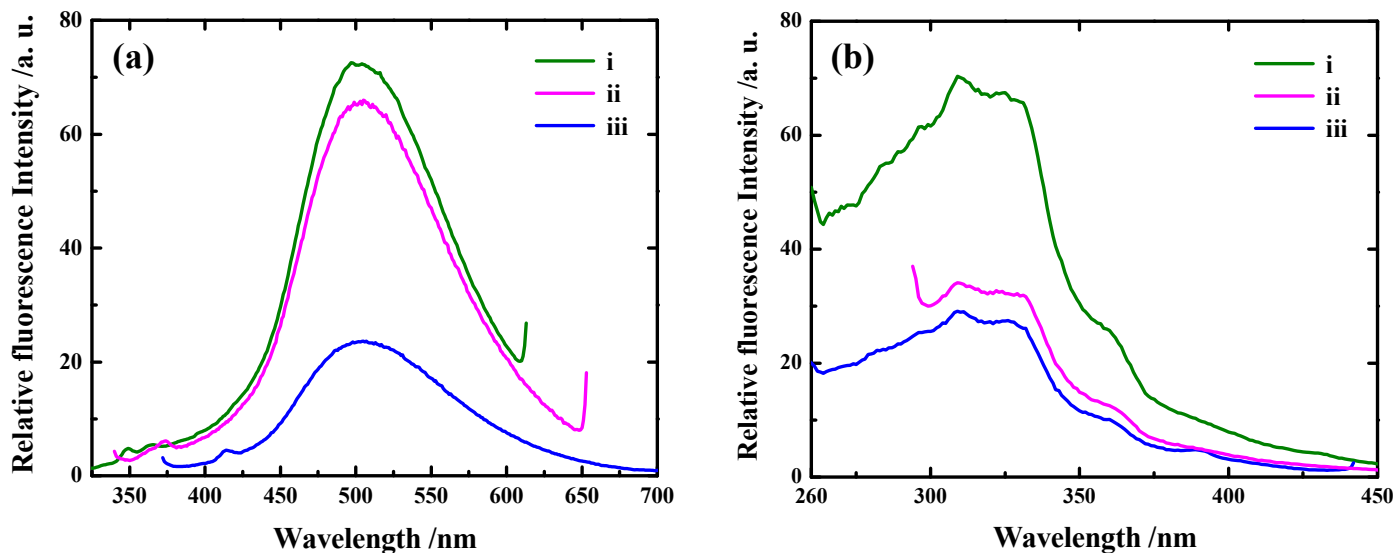


Fig. S9. (a) Emission spectra of TPM-MOP nanoparticle (TMN) dispersion at different excitation wavelengths: (i) $\lambda_{\text{exc}} = 311$, (ii) 331 and (iii) 363 nm. (b) Excitation spectra of TMN dispersion at different emission wavelengths: (i) $\lambda_{\text{em}} = 505$, (ii) 580 and (iii) 450 nm.

Rhodamine 6G coated nanoparticle dispersion: Emission and excitation spectra of Rhodamine 6G loaded nanoparticle (TMN-RG) dispersions were also found to be independent of excitation and emission wavelengths respectively. Excitation at any wavelength in the absorption band of TPM-MOP nanoparticles in TMN-RG dispersion resulted in significant quenching of fluorescence from polymer nanoparticles, thus demonstrating efficient energy transfer from nanoparticles to surface bound Rhodamine 6G dye molecules.

Approximate percentage of Rhodamine 6G content ($\sim 0.1\%$, w/w) in the TMN-RG dispersion was estimated by calculating the concentration of dye in the dispersion using its molar extinction coefficient in water and the polymer content of the nanoparticle dispersion.

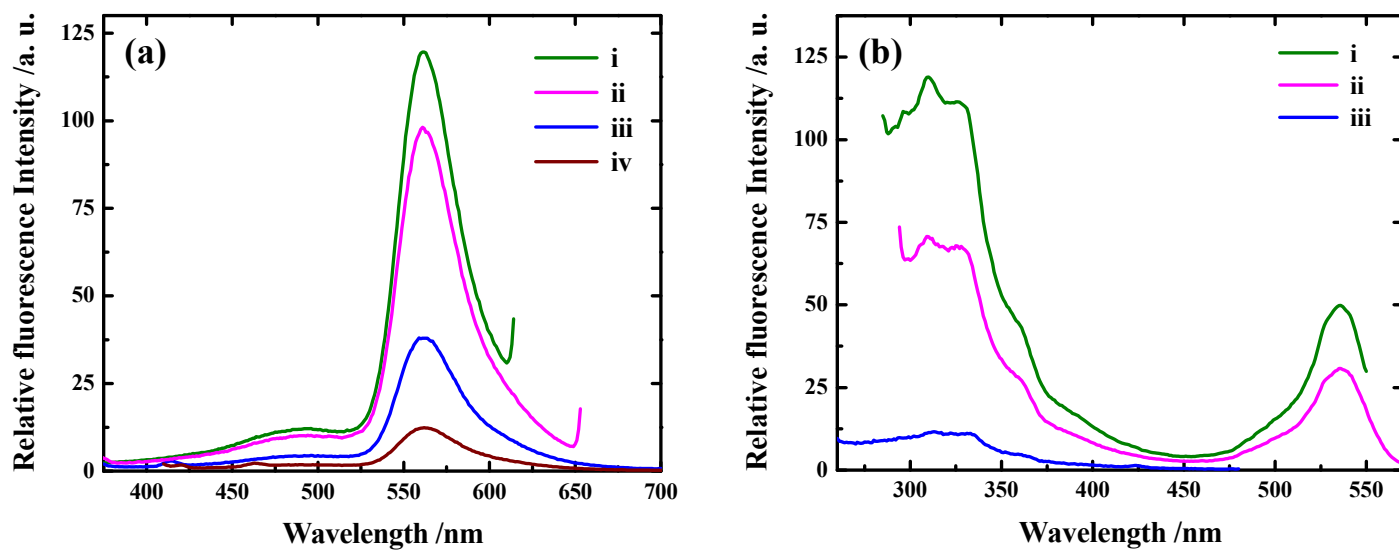


Fig. S10. (a) Emission spectra of Rhodamine 6G loaded TPM-MOP nanoparticle dispersion (TMN-RG) at different excitation wavelengths: (i) $\lambda_{\text{exc}} = 311$, (ii) 331, (iii) 363 and (iv) 400 nm. (b) Excitation spectra of TMN-RG at different emission wavelengths: (i) $\lambda_{\text{em}} = 561$, (ii) 580 and (iii) 495 nm.

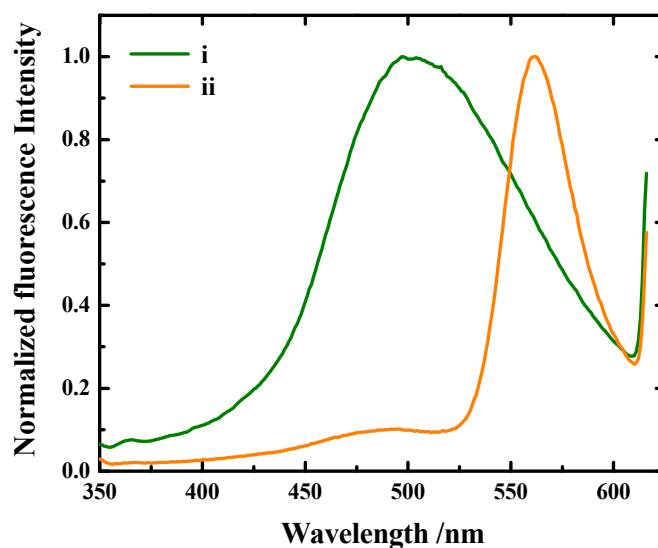


Fig. S11. Normalized emission spectra of TPM-MOP nanoparticle dispersion (TMN) and Rhodamine 6G loaded nanoparticle dispersion (TMN-RG): (i) TMN, $\lambda_{\text{exc}} = 311$, (ii) TMN-RG, $\lambda_{\text{exc}} = 311$.

References

1. M. Grimm, B. Kirste and H. Kurreck, *Angew. Chem. Int. Ed. Engl.*, 1986, **25**, 1097.
2. H. Lim and J. Y. Chang, *Macromolecules*, 2010, **43**, 6943.
3. E. Stöckel, X. Wu, A. Trewin, C. D. Wood, R. Clowes, N. L. Campbell, J. T. A. Jones, Y. Z. Khimyak, D. J. Adams and A. I. Cooper, *Chem. Commun.*, 2009, 212.
4. J. Pecher, J. Huber, M. Winterhalder, A. Zumbusch and S. Mecking, *Biomacromolecules*, 2010, **11**, 2776.
5. J. N. Demas and G. A. Crosby, *J. Phys. Chem.* 1971, **75**, 991.